RSC Advances

ROYAL SOCIETY OF CHEMISTRY

www.rsc.org/advances

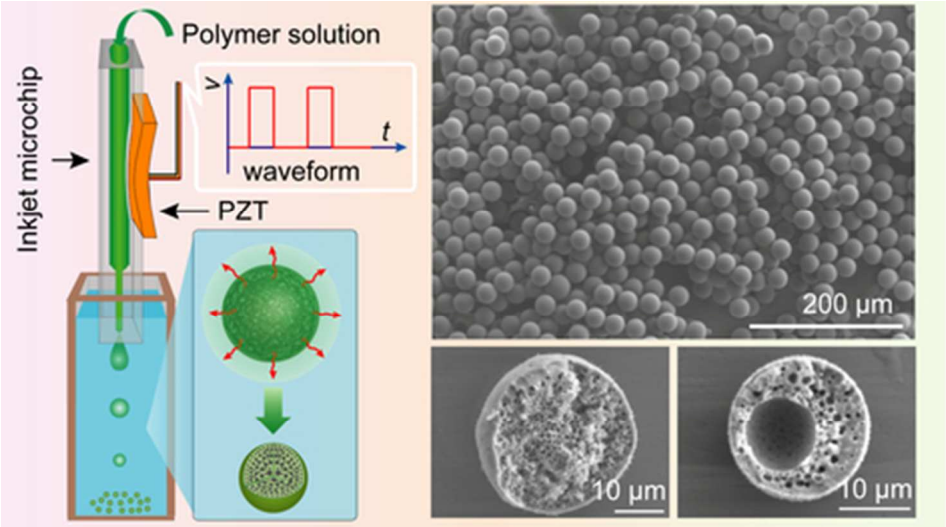

A piezoelectric drop-on-demand (DOD) inkjet microchip with its nozzle immersed in organic phase was used to generate monodisperse porous polymer particles.
39x22mm (300 x 300 DPI)

Journal Name

RSCPublishing

ARTICLE

Generation of controlled monodisperse porous polymer particles by dipped inkjet injection

Cite this: DOI: 10.1039/xoxxoooooox

Jianmin Yang, Daisuke Katagiri, Sifeng Mao, Hulie Zeng,* Hizuru Nakajima and Katsumi Uchiyama*

Received ooth January 2012,
Accepted ooth January 2012

DOI: 10.1039/xoxxoooooox

www.rsc.org/

A straightforward approach for the preparation of monodisperse porous polymer particles by inkjet technology is reported. Uniform droplets of an aqueous polymer solution were ejected from an inkjet, the nozzle of which was immersed in an organic phase. The subsequent dehydration of the droplets by solvent extraction resulted in the formation of porous polymer microspheres. Particles with a narrow size distribution could be obtained using the present system in a single step. Parameters for polymer droplet generation in organic phase, including polymer properties, organic solvent, and inkjet waveform, were investigated. The relationship between the final particle diameter and the initial polymer droplet size was also examined. The diameters of particles could be precisely controlled by changing the waveform exerted on the inkjet, thus producing particles with diameters in the range of 15 μm ~ 60 μm with a coefficient of variation (CV) in the range of 2.7% ~ 4.8%. It was also possible to produce hollow porous polymer particles by simply decreasing the concentration of the polymer solution. The results demonstrate the merit of the inkjet-based method for the generation of monodisperse porous polymer particles. The method has the potential for producing functional polymer particles via the incorporation of functional or smart materials.

Introduction

With benefit of a large surface area, low density and ease of incorporation of functional groups, porous polymer particles have great potential for use in coatings, chromatography, catalytic supports, sensing, medical imaging, controlled drug release, etc.[1-4] In particular, porous polymer particles with a uniform size distribution have attracted great interest because this represents an enhancement in terms of their application. For example, use of monodisperse porous polymer particles results in a significant improvement in separation efficiency in liquid chromatography.[5] It has also been reported that drug payloads and release rate kinetics are directly dependent on both the morphology and size of these carriers.[6-8]

Conventional methods for polymer particle production include solid colloid templating, suspension polymerization, spray drying, emulsion polymerization, and seeded emulsion polymerization.[9-11] However techniques involve multiple steps, can be time consuming and a large size distribution is usually observed. All of these points narrow the range of application for such materials. As a result, various techniques, mostly based on the fluid dynamics, have been explored to generate uniform polymer particles in a simplified and more straightforward manner.[12-16] Among them, microfluidic-based droplet generation methods, in which droplets are ejected in an immiscible organic or aqueous phase, have been proved to be the most efficient technique for producing monodisperse polymeric microparticles.[17,18] Polymeric microparticles with controllable sizes and shapes have been fabricated on T-junction, flow-focusing, or co-flow geometry platforms.[19-22] Unfortunately, as clearly pointed out in some reports,[19,23,24] the organic solvent sometimes causes poly(dimethyl siloxane) (PDMS) based microfluidic devices to undergo swelling and contamination cannot be ignored. Thus, alternative materials to PDMS for the microfluidic platform have been proposed to address this issue.[23,25,26] However, so far, the current large scale production of monodisperse microspheres utilizing microfluidic or other apparatus still need the accurate manipulation technology and complicated supporting device, which should be performed by the specialists under strictly controlled experimental conditions.

Recently, inkjet printing has attracted considerable interest in this area, because it permits droplets to be manipulated the picoliter level for the resulting droplets to be precisely dispersed with spatial and temporal control. Taking advantage of easily controlling the droplet size and velocity of a fluid by changing the actuation pulse waveform, the piezoelectric drop-on-demand (DOD) inkjet, which is widely used in both industrial and scientific area settings, represents an ideal approach to solving this problem.[27-33] In the field of particle fabrication, it initially served as an alternative technique to spray drying technology which pioneered a new manufacturing technique known as inkjet spray drying or jetting technology. The size and morphology of controllable particles can be explained by a mechano-electrically governed mechanism.[34-38] However, it should be noted that these particles were usually prepared with the inkjet nozzle located above the solvent medium, in which the droplet is first released into air. The particle is then formed after the droplet falls into the solvent medium. Thus, the force of the collision between droplets and the solvent interface resulted in particles with

an irregular morphology. Additionally, the size of particles was found to be in a narrow adjustable range which resulted from the limited injection conditions for ink-jetting in air. To our knowledge, the generation of porous polymer particles with a well-defined sphere morphology by inkjet technology has never been reported.

In this paper, a straightforward approach based on inkjet technology for the preparation of monodisperse porous polymer particles is reported. A DOD inkjet injector with its head immersed in an organic continuous phase was used to generate monodisperse microparticles. By finely tuning the waveform applied to the piezoelectric transducer on the inkjet microchip, an aqueous polymer solution was easily ejected from the injector into the organic phase. A polymer droplet was subsequently generated in the organic continuous phase. Due to the extraction of water from the droplet by the organic phase and accompanied by the self-assembling property of the polymer molecule, the droplet was transformed into porous particle within a short period. By integrating the inkjet technique with "droplet-to-particle" synthesis approaches,[39-41] uniform porous polymer particles were fabricated in a one step procedure, within a few minutes. The sizes of particles were precisely controlled from 15 μm to 60 μm with a coefficient of variation (CV) ranging from 2.7% to 4.8%. Additionally, hollow porous polymer particles with various dimensions were also produced by the present system through changing the concentration of the polymer solution.

Experimental

Reagents and solutions

Sodium poly(styrenesulfonate) (NaPSS, 30 wt% in water) with an average molecular weight of 70 kg/mol was purchased from Sigma-Aldrich (St. Louis, Missouri, USA). Sodium dodecyl sulfate (SDS) and ethanol were purchased from Wako Pure Chemical (Osaka, Japan). Serial dilutions of NaPSS (2.5 wt%, 5 wt%, 7.5 wt%, 10 wt% and 15 wt%) containing 10 mM sodium dodecyl sulfate (SDS) were used as the polymer solutions. 1-Butanol was obtained from Kanto Chemical (Tokyo, Japan) and was used as the extraction solvent. The surface tension of each solution was measured using a Du Nouy Tensiometer (Itoh Seisakusho, Ltd., Tokyo, Japan), and the viscosity was analyzed by an Ubbelohde-type viscometer (Sibata Scientific Technology Ltd., Tokyo, Japan). Deionized water was obtained from a Direct-Q™5 Nihon Millipore ultrapure water system (Tokyo, Japan).

Equipment and procedure

The equipment used for producing porous polymer particles formation is illustrated in Fig. 1b. It is composed of a piezoelectric DOD inkjet microchip (Fuji Electric, Tokyo, Japan) and an extraction solvent-filled glass cell. The nozzle of the inkjet microchip was immersed in the extraction solvent (about 3 mm depth from the tip). As described in our previous reports,[42,43] the inkjet microchip with a nozzle diameter of about 80 μm was controlled by a laboratory-fabricated circuit and software. The polymer solution loaded in the inkjet microchip was pressed by the bent piezoelectric ceramic, and the droplets were then ejected from the nozzle into the extraction solvent. Afterwards, the droplets were gradually transformed into porous particles with the water molecules in polymer solution diffusing into the extraction phase. Finally, all particles sank down on the bottom of the glass cell. Droplet sizes were varied by changing the driving voltage and pulse width. The particles with extraction solvent were pipetted onto a glass slide and dried overnight in a desiccator.

Droplet measurement and particle characterization

The process of the injections was recorded on a high speed camera (Keyence VW-9000, Osaka, Japan). Still images were generated from the videos using a VW-9000 Motion Analyzer, and the droplet sizes in the still images were analyzed. The mean droplet size for each injection condition was calculated from measurements of 30 droplets. An optical microscope, Olympus system microscope BX53 equipped with a digital camera DP73 (Olympus Co., Tokyo, Japan), was used to study the diameter of the resulting particles. To determine the size distribution of the particles, at least 250 microspheres in each sample were measured by the measuring software on the optical microscope. The surface and internal morphology of particles were examined by means of a scanning electron microscope (SEM) system (S-3400N, Hitachi Co., Tokyo, Japan). Particles were coated with a gold layer using a sputter coater (SC-701, Sanyu Denshi Co., Tokyo, Japan) prior to obtaining the SEM images. For the morphology of internal structures, the particles were squeezed to split by glass plate before SEM characterization.

Results and discussion

Generation of monodisperse polymer droplets

The procedure employed to fabricate porous polymer microparticles combined the generation of monodisperse droplets of polymer aqueous solution using inkjet microchip, with subsequent mutual diffusion to form porous particles. The fabrication of porous polymer microparticles was performed by using an inkjet microchip, with its nozzle immersed in an organic phase. As schematically illustrated in Fig. 1a, porous particles were formed by the generation of monodisperse aqueous polymer solution droplets followed by their mutual diffusion in an organic phase. Sodium poly(styrenesulfonate) (NaPSS), a biocompatible material, has been widely used as drug carrier in controlled-release preparations.[44-46] Meanwhile, the high self-assembly properties of NaPSS make it convenient for the formation of polymer particles by means of a simple process.[39] Therefore, an NaPSS aqueous solution was selected as a model polymer solution for producing microparticles in this work. In order to extract the water in the polymer solution to form polymer particles, the extraction solvent should be miscible with water and immiscible with respect to NaPSS. However, water-miscible solvents such as, methanol, ethanol and acetone, failed to form spherical particles. The reason for this is that the rapid solvent exchange at the interphase hindered particle formation. Consequently, 1-butanol, partially miscible in water was chosen as the extraction solvent, which permitted robust and well-defined spherical particles to be generated.

Higher ratios of viscosity to surface tension can prevent satellite droplet production in ink-jetting. Thus, sodium dodecyl sulfate (SDS) was added to the polymer solution to a final concentration of 10 mM. In this situation, the SDS not only increases fluid viscosity, but also reduces surface tension. However, a higher viscosity would increase the difficulty of ejection and it would be necessary to apply a larger pulse voltage to the actuator. From our experimental results, the inkjet failed to inject when the concentration of NaPSS exceeded 15 wt%, in which the viscosity was 6.8 mPa s. Therefore, aqueous NaPSS solutions with concentrations from 2.5 wt% to 15 wt% containing 10 mM SDS were used for droplet generation. The density, viscosity and surface tension of each fluid is listed in Table S1†.

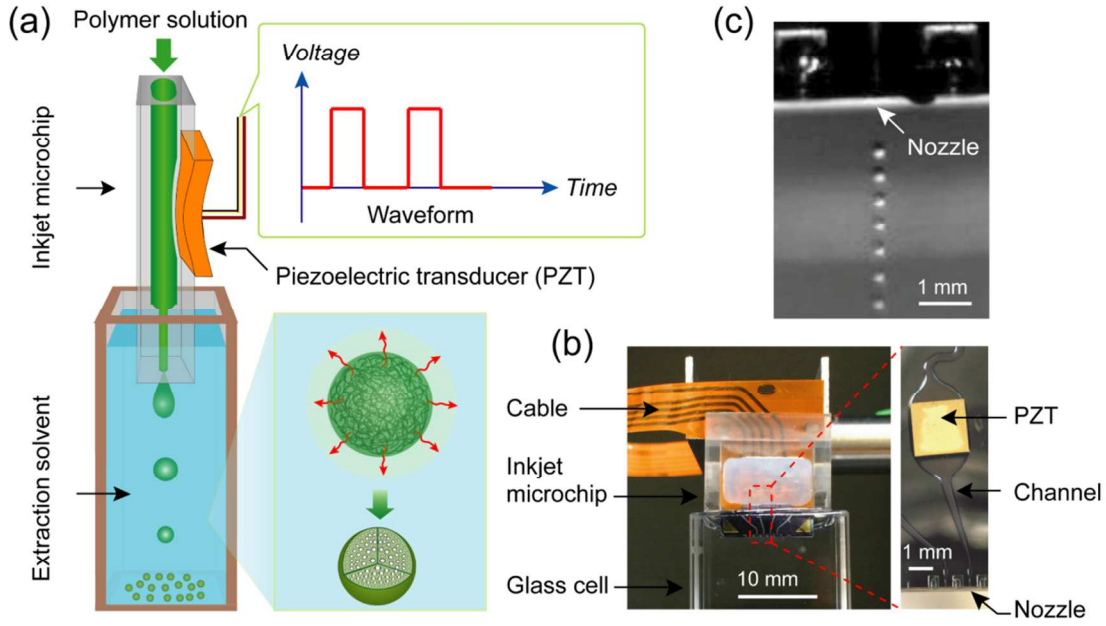

Fig. 1 (a) Schematic illustration of the experimental set-up designed to produce monodisperse porous polymer particles. The enlarged diagram indicates the porous polymer particle formation mechanism in the extraction solvent. (b) The digital photograph of the experimental set-up. The enlarge photograph is the channel structure of inkjet microchip. (c) Typical photograph of monodisperse polymer solution droplets jetting into the extraction solvent, droplets sizes ≈ 180 μm. The concentration of NaPSS was 15 wt%. All procedures were performed at 25 °C.

Fig. 1c shows an image of the droplet of the polymer solution ejected into 1-butanol. Monodisperse droplets were obtained one by one at a frequency of 5 droplets per second (5 Hz). Details of the process can be found in the Supplementary Information Video S1†, which was recorded by a high speed camera. The representative single polymer droplet generation process in 1-butanol is vividly displayed in Fig. 2 in sequential images, and the corresponding video can be found in Supplementary Information, Video S2†. The polymer solution emerged at the nozzle when the driving voltage was applied on the inkjet actuator. The solution then moved forward to form a cylindrical pillar followed by the division of the pillar after hundreds of microseconds. Finally, a well-defined spherical droplet was spontaneously generated by shrinking, which induced by the surface tension. And the droplet could remain the most stable spherical state. The entire process is complete in 2 ms in the case of a high velocity (the initial speed was about 500 mm/s). After that, the speed decreased, eventually reaching its sedimentation velocity. The sedimentation velocity was detected at 2 mm/s. Since the density of the polymer solution was slightly larger than that of 1-butanol, the droplet sank to the bottom of the glass cell by gravity.

Unlike the conventional microchip-based microfluidic approaches, a carrier phase for droplet generation is not necessary in inkjet technology. Herein, the polymer solution is directly injected into a continuous phase (or extraction phase) on demand, which minimizes the risk of contamination from additional reagents. The frequency of droplet ejection was controlled by the inkjet driver. However, due to the slow sedimentation velocity driven by gravity, the maximum frequency of the method was 10 Hz. Moreover, the snap-off and re-coil of the polymer solution would entrainment a small amount of extraction solvent in to the nozzle of inkjet microchip. However, the entrainment effect could be negligible in the dipped inkjet injection because the interval of each injection (100-200 ms) was extremely short compared to the slow extraction process of solvent.

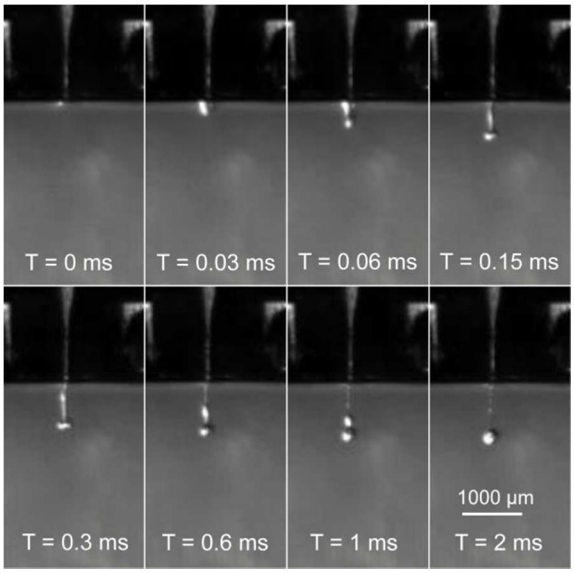

Fig. 2 Photos of the aqueous polymer solution droplet generation process in 1-butanol. The injection condition set as driving voltage was 50 V with 40 μs pulse width, droplet size ≈ 210 μm. The concentration of NaPSS was 15 wt%.

Effect of injection condition on droplet size

The sizes of droplet were mainly depending on the characteristics of the fluid, diameter of inkjet nozzle, and the waveform applied to the

inkjet actuator. The droplet is generated by the waveform applied to the piezo-element on an inkjet microchip. Thus, droplet size is easily adjusted via changing the driving voltage and pulse width. Injection conditions for monodisperse polymer droplet generation in 1-butanol were investigated with the polymer concentration set at 15 wt%. On the other hand, the dependence of injection condition on droplet size was fitted based on actual measurement data. As can be seen in Fig. 3, monodisperse droplets were generated in 1-butanol with a driving voltage ranging from 15 V to 80 V, and with a pulse width from 15 μs to 90 μs. Herein, to avoid damage to the inkjet microchip by a high voltage, the maximum driving voltage was set as 80 V. As has been demonstrated in previous reports,[47] the size of the droplet injected into air is linearly dependent on the driving voltage, but showed a more complicated behaviour with changing pulse width. A similar behaviour was observed when the droplet entered the liquid phase. Generally, the sizes of droplets increased with increasing driving voltage and pulse width, and the size distribution ranged from 80 μm to 240 μm. In addition, the injection conditions for polymer concentrations ranging from 2.5 wt% to 10 wt% were also investigated (Fig. S1†). The results indicated that both injection conditions and the adjustable range of droplet size were significantly larger than the monodisperse droplet generated in air (Fig. S2†).

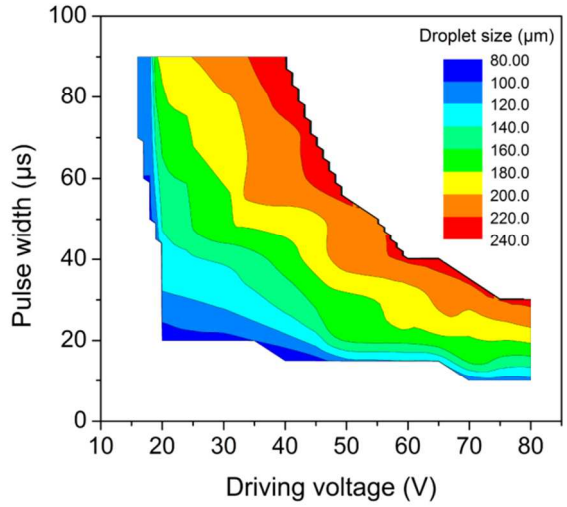

Fig. 3 The scope of injection conditions for monodisperse aqueous polymer solution droplet generation in 1-butanol and droplet size distribution. The concentration of NaPSS was 15 wt%. Colored regions show the possible scopes for monodisperse droplet generation. Various colors represent the size distribution of droplet.

Porous particle formation and characterization

Fig. 4a and b shows SEM images of resulting polymer particles for a NaPSS concentration of 15 wt%. Well-defined spherical polymer particles with a uniform size distribution and a smooth surface were obtained. Particle formation was completed in a single step by the "droplet-to-particle" approach. The particle formation process was triggered when the NaPSS-water droplet was injected into 1-butanol. Due to the extraction of the water from the droplet into 1-butanol, the size of the droplet shrank and was subsequently transformed into particles by virtue of the self-assembling property of NaPSS molecules. Particles with controllable diameters ranging from 20 μm to 60 μm were prepared (Fig. S3†). The interior structures of the particles were characterized by SEM after crushing the particle with a glass slide. Both small (20 μm) and larger diameter (30 μm) particles showed a porous structure inside shelled surface (see Fig. 4c and d). The pore size is about tens to hundreds of nanometers, and the density of porosity appears to be slightly increased toward the center of the particle.

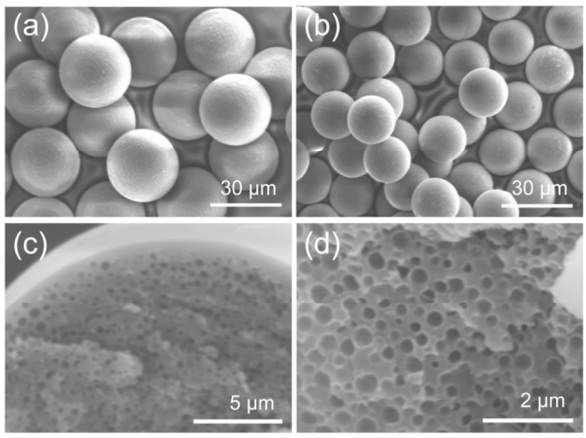

Fig. 4 SEM images of monodisperse polymer particles with diameter of (a) 30 μm and (b) 20 μm. The interior structure of particles with diameters of (c) 30 μm and (d) 20 μm. The concentration of NaPSS was 15 wt%. The injection condition for (a) and (c) the driving voltage was 30 V with 30 μs pulse width, for (b) and (d) the driving voltage was 20 V with 20 μs pulse width.

The monodispersity of particles was evaluated by the mean particle size and the diameter CV. The CV is defined by CV = (σ/μ) × 100, where σ is the standard deviation of the diameter, and μ is the average diameter. The diameters of the particle were measured after the resulting particle was dried overnight in a desiccator. At least 250 particles in each sample were measured using dimensional measurement software on the optical microscope. Fig. 5 shows the size distribution of particles with diameters ranging from 15 μm to 60 μm. All size categories particles have narrow size distributions with a CV value in the range of 2.7%–4.8% (Table S2†). The results confirm that the monodisperse porous polymer particles were successfully prepared using the present method. Meanwhile, from the point view of size distribution, the present method is significantly superior to previous reports [36-38].

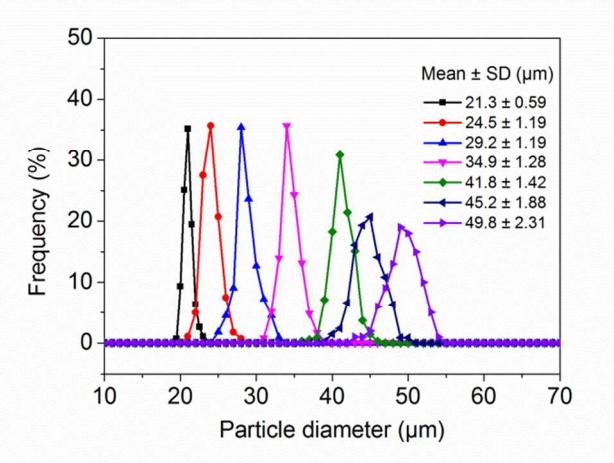

Fig. 5 Size distribution of the polymer particles. The concentration of NaPSS was 15 wt%.

Hollow core–shell structure particles

Hollow core–shell structures of porous particles were generated by varying the concentration of the polymer solution. As shown in Fig.

6, particles produced using a concentration of NaPSS of 2.5 wt% and 5 wt% had a hollow structure. On the one hand, the volume ratio of hollow core to shell was increased with decreasing polymer concentration. On the other hand, the average pore size was decreased as the initial polymer concentration was increased. Meanwhile, a dimple was found on these particles. This is attributed to the partial collapse of the surface caused by the hollow structure. The mechanism of for hollow core formation can be attributed to the diffusion of polymer molecules.[48] During the generation of a polymer droplet in the extraction phase, polymer molecules in the internal droplets diffused to the interface of the droplets and formed the shell. As these molecules gradually being adsorbed onto the inner surface of shell, a polymer molecule vacant area occurred in the center of droplet. And then a hollow core structure was generated in the resulting particles. However, the porous internal structure was generated as the concentration of the polymer solution was increased. The reason is that the increased viscosity of the polymer solution with a high concentration inhibited the diffusion of the polymer molecules inside the droplet. Therefore, the internal structures became porous when the NaPSS concentrations were higher than 7.5 wt% and 10 wt% (Fig. S4†).

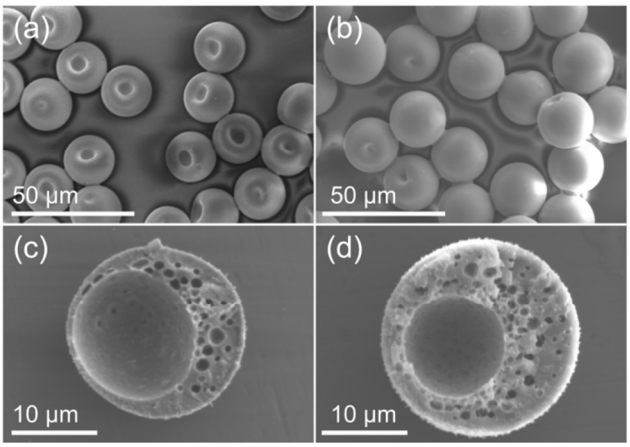

Fig. 6 SEM images of surface and interior structure of particles obtain from various polymer concentrations. The polymer concentration was (a, c) 2.5 wt% and (b, d) 5.0 wt%. The injection condition for (a) and (c) the driving voltage was 20 V with 40 μs pulse width, for (b) and (d) the driving voltage was 20 V with 30 μs pulse width.

Relationship of droplet size and particle diameter

The effects of the initial droplet size and polymer concentration on the final particle size were also investigated, and the results are shown in Fig. 7. An approximately linear relationship between the final particle size and the initial droplet size was observed, and the slope of the plot varied with a change in polymer concentration. Overall, the particle diameter was smaller than the droplet size, indicating that the volume shrinkage of the droplets is induced by solvent diffusion. The ratios of droplet size to particle diameter were 6.40 ± 0.14, 6.06 ± 0.17, 5.59 ± 0.08, 5.36 ± 0.13, and 4.09 ± 0.13, with the polymer concentrations of 2.5%, 5%, 7.5%, 10%, and 15%, respectively. The results suggest that the particle diameter can be estimated from the initial droplet size and polymer concentration. While, the initial droplet size was dependent on the waveform applied to the inkjet actuator. Therefore, the diameter of porous polymer particles can be easily controlled with the approach described herein.

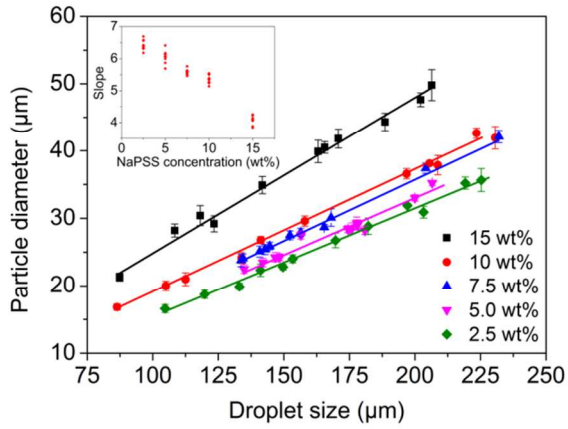

Fig. 7 Effect of initial droplet size and polymer concentration on the diameter of the final particle. The slope is indicated in the inset figure.

Conclusions

Porous polymer particles with a narrow size distribution were directly fabricated by dipped inkjet injection. Particles with diameters in the range of 15 μm to 60 μm could be precisely controlled by fine tuning the waveform applied to the inkjet microchip. In addition, hollow porous polymer particles were also obtained when the concentration of the polymer solution was decreased. The resulting particles in this size range represent be promising candidates for use as functional, optical, ultrasound contrast agents, and coating materials. Smaller particle could be obtained when an inkjet with a smaller size nozzle is used. High-throughput production could be easily achieved by fabricating a multi-nozzle inkjet setup via adding the number of nozzles and cables.[49] We believe that the inkjet-based approach described here represents a potentially universal platform for the production of monodisperse porous polymer particles, which could be carried out in common laboratory or industrial settings.

Acknowledgements

This work was financially supported by the High Technology Research Project by Tokyo Metropolitan Government.

Notes and references

Department of Applied Chemistry, Graduate School of Urban Environmental Sciences, Tokyo Metropolitan University, Minamiohsawa, Hachioji, Tokyo 192-0397, Japan. Fax: +81-42-6772821; Tel: +81-42-6772835. E-mail: zeng-hulie@tmu.ac.jp, uchiyama-katsumi@tmu.ac.jp.

† Electronic Supplementary Information (ESI) available. See DOI: 10.1039/b000000x/

1 R. Haag and S. Roller, *Top. Curr. Chem.*, 2004, **242**, 1-42.
2 D. A. Edwards, J. Hanes, G. Caponetti, J. Hrkach, A. Ben-Jebria, M. L. Eskew, J. Mintzes, D. Deaver, N. Lotan and R. Langer, *Science*, 1997, **276**, 1868-1871.
3 R. Hayes, A. Ahmed, T. Edge and H. Zhang, *J. Chromatogr. A*, 2014, **1357**, 36-52.

4 H. Zhang, D. Liu, M. A. Shahbazi, E. Mäkilä, B. Herranz-Blanco, J. Salonen, J. Hirvonen and H. A. Santos, *Adv. Mater.*, 2014. **26**, 4497-4503.
5 L. A. Wiest, D. S. Jensen, C. H. Hung, R. E. Olsen, R. C. Davis, M. A. Vail, A. E. Dadson, P. N. Nesterenko and M. R. Linford, *Anal. Chem.*, 2011, **83**, 5488-5501.
6 D. S. Kohane, *Biotechnol. Bioeng.*, 2007, **96**, 203-209.
7 W. J. Duncanson, T. Lin, A. R. Abate, S. Seiffert, R. K. Shah and D. A. Weitz, *Lab Chip*, 2012, **12**, 2135-2145.
8 C. Berkland, K. K. Kim and D. W. Pack, *J. Control. Release*, 2001, **73**, 59-74.
9 M. T. Gokmen and F. E. Du Prez, *Prog. Polym. Sci.*, 2012, **37**, 365-405.
10 J. Tan, C. Li, J. Zhou, C. Yin, B. Zhang, J. Gu and Q. Zhang, *Rsc Adv.*, 2014, **4**, 13334-13339.
11 U. Jeong, S. H. Im, P. H. C. Camargo, J. H. Kim and Y. Xia, *Langmuir*, 2007, **23**, 10968-10975.
12 T. Nakashima, M. Shimizu and M. Kukizaki, *Adv. Drug Deliv. Rev.*, 2000, **45**, 47-56.
13 J. H. Kim, T. Y. Jeon, T. M. Choi, T. S. Shim, S. H. Kim and S. M. Yang, *Langmuir*, 2014, **30**, 1473-1488.
14 J. T. Wang, J. Wang and J. J. Han, *Small*, 2011, **7**, 1728-1754.
15 R. Liu, G. Ma, F. T. Meng and Z. G. Su, *J. Control. Release.*, 2005, **103**, 31-43.
16 X. D. He, X. W. Ge, H. R. Liu, M. Z. Wang and Z. C. Zhang, *Chem. Mater.*, 2005, **17**, 5891-5892.
17 J. I. Park, A. Saffari, S. Kumar, A. Günther and E. Kumacheva, *Annu. Rev. Mater. Res.*, 2010, **40**, 415-443.
18 D. Dendukuri and P. S. Doyle, *Adv. Mater.*, 2009, **21**, 4071-4086.
19 A. S. Utada, E. Lorenceau, D. R. Link, P. D. Kaplan, H. A. Stone and D. A. Weitz, *Science*, 2005, **308**, 537-541.
20 D. Liu, H. Zhang, B. Herranz-Blanco, E. Mäkilä, V. P. Lehto, J. Salonen, J. Hirvonen and H. A. Santos, *Small*, 2014, **10**, 2029-2038.
21 T. Nisisako, T. Torii and T. Higuchi, *Chem. Eng. J.,* 2004, **101**, 23-29.
22 Q. Xu, M. Hashimoto, T. T. Dang, T. Hoare, D. S. Kohane, G. M. Whitesides, R. Langer and D. G. Anderson, *Small*, 2009, **5**, 1575-1581.
23 S. W. Choi, I. W. Cheong, J. H. Kim and Y. Xia, *Small*, 2009, **5**, 454-459.
24 S. Takeuchi, P. Garstecki, D. B. Weibel and G. M. Whitesides, *Adv. Mater.*, 2005, **17**, 1067-1072.
25 E. Quevedo, J. Steinbacher and D. T. McQuade, *J. Am. Chem. Soc.*, 2005, **127**, 10498-10499.
26 M. T. Gokmen, W. Van Camp, P. J. Colver, S. A. F. Bon and F. E. Du Prez, *Macromolecules*, 2009, **42**, 9289-9294.
27 M. Singh, H. M. Haverinen, P. Dhagat and G. E. Jabbour, *Adv. Mater.*, 2010, **22**, 673-685.
28 E. B. Secor, P. L. Prabhumirashi, K. Puntambekar, M. L. Geier and M. C. Hersam, *J. Phys. Chem. Lett.*, 2013, **4**, 1347-1351.
29 R. D. Boehm, P. R. Miller, J. Daniels, S. Stafslien and R. J. Narayan, *Mater. Today*, 2014, **17**, 247-252.
30 F. Torrisi, T. Hasan, W. Wu, Z. Sun, A. Lombardo, T. S. Kulmala, G. W. Hsieh, S. Jung, F. Bonaccorso, P. J. Paul, D. Chu and A. C. Ferrari, *ACS Nano*, 2012, **6**, 2992-3006.
31 Y. Sun, X. Zhou and Y. Yu, *Lab Chip*, 2014, **14**, 3603-3610.
32 S. Hauschild, U. Lipprandt, A. Rumplecker, U. Borchert, A. Rank. R. Schubert and S. Förster, *Small*, 2005, **1**, 1177-1180.
33 P. J. Smith and A. Morrin, *J. Mater. Chem.,* 2012, **22**, 10965-10970.
34 S. Iwanaga, N. Saito, H. Sanae and M. Nakamura, *Colloids Surf. B*, 2013, **109**, 301-306.
35 E. Tekin, P. J. Smith and U. S. Schubert, *Soft Matter*, 2008, **4**, 703-713.
36 H. Tamura, K. Kadota, Y. Shirakawa, Y. Tozuka, A. Shimosaka and J. Hidaka, *Adv. Powder Technol.*, 2014, **25**, 847-852.
37 K. Kadota, H. Tamura, Y. Shirakawa, Y. Tozuka, A. Shimosaka and J. Hidaka, *Chem. Eng. Res. Des.*, 2014, **92**, 2461-2469.
38 D. P. Go, D. J. E. Harvie, N. Tirtaatmadja, S. L. Gras and A. J. O'Connor, *Part. Part. Syst. Char.*, 2014, **31**, 685-698.
39 T. Watanabe, C. G. Lopez, J. F. Douglas, T. Ono and J. T. Cabral, *Langmuir*, 2014, **30**, 2470-2479.
40 N. Hakimi, S. S. Tsai, C. H. Cheng and D. K. Hwang, *Adv. Mater.*, 2014, **26**, 1393-1398.
41 Q. Qian, X. Huang, X. Zhang, Z. Xie and Y. Wang, *Angew. Chem. Int. Ed. Engl.*, 2013, **52**, 10625-10629.
42 H. Zeng, Y. Weng, S. Ikeda, Y. Nakagawa, H. Nakajima and K. Uchiyama, *Anal. Chem.*, 2012, **84**, 10537-10542.
43 J. Yang, H. Zeng, S. Xue, F. Chen, H. Nakajima and K. Uchiyama, *Anal. Methods*, 2014, **6**, 2832-2836.
44 J. Zhang, C. Li, Y. Wang, R. X. Zhuo and X. Z. Zhang, *Chem. Commun.*, 2011, **47**, 4457-4459.
45 L. Xie, W. Tong, D. Yu, J. Xu, J. Li and C. Gao, *J. Mater. Chem.*, 2012, *22*, 6053-6060.
46 J. Zhou, M. V. Pishko and J. L. Lutkenhaus, *Langmuir*, 2014, **30**, 5903-5910.
47 N. Reis, C. Ainsley and B. Derby, *J. Appl. Phys.*, 2005, **97**, 094903.
48 T. Suzuki, A. Osumi, and H. Minami, *Chem. Commun.,* 2014, **50**, 9921-9924.
49 K. C. Patel and X. D. Chen, *Asia-Pac. J. Chem. Eng.*, 2007, **2**, 415-430.

